

11-1-2010

Genome structures and halophyte-specific gene expression of the extremophile *thellungiella parvula* in comparison with *Thellungiella salsuginea* (*Thellungiella halophila*) and *arabidopsis*

Dong Ha Oh

University of Illinois at Urbana-Champaign

Maheshi Dassanayake

University of Illinois at Urbana-Champaign

Jeffrey S. Haas

University of Illinois at Urbana-Champaign

Anna Kropornika

University of Illinois at Urbana-Champaign

Chris Wright

University of Illinois at Urbana-Champaign

See next page for additional authors

Follow this and additional works at: https://digitalcommons.lsu.edu/biosci_pubs

Recommended Citation

Oh, D., Dassanayake, M., Haas, J., Kropornika, A., Wright, C., d'Urzo, M., Hong, H., Ali, S., Hernandez, A., Lambert, G., Inan, G., Galbraith, D., Bressan, R., Yun, D., Zhu, J., Cheeseman, J., & Bohnert, H. (2010). Genome structures and halophyte-specific gene expression of the extremophile *thellungiella parvula* in comparison with *Thellungiella salsuginea* (*Thellungiella halophila*) and *arabidopsis*. *Plant Physiology*, 154 (3), 1040-1052. <https://doi.org/10.1104/pp.110.163923>

This Article is brought to you for free and open access by the Department of Biological Sciences at LSU Digital Commons. It has been accepted for inclusion in Faculty Publications by an authorized administrator of LSU Digital Commons. For more information, please contact ir@lsu.edu.

Authors

Dong Ha Oh, Maheshi Dassanayake, Jeffrey S. Haas, Anna Kropornika, Chris Wright, Matilde Paino d'Urzo, Hyewon Hong, Shahjahan Ali, Alvaro Hernandez, Georgina M. Lambert, Gunsu Inan, David W. Galbraith, Ray A. Bressan, Dae Jin Yun, Jian Kang Zhu, John M. Cheeseman, and Hans J. Bohnert

Genome Structures and Halophyte-Specific Gene Expression of the Extremophile *Thellungiella parvula* in Comparison with *Thellungiella salsuginea* (*Thellungiella halophila*) and *Arabidopsis*^{1[W]}

Dong-Ha Oh^{2*}, Maheshi Dassanayake², Jeffrey S. Haas, Anna Kropornika, Chris Wright, Matilde Paino d'Urzo, Hyewon Hong, Shahjahan Ali, Alvaro Hernandez, Georgina M. Lambert, Gunsu Inan, David W. Galbraith, Ray A. Bressan, Dae-Jin Yun, Jian-Kang Zhu, John M. Cheeseman, and Hans J. Bohnert

Department of Plant Biology (D.-H.O., M.D., A.K., H.H., J.M.C., H.J.B.), Office of Networked Information Technology, School of Integrative Biology (J.S.H.), Center for Comparative and Functional Genomics (C.W., S.A., A.H., H.J.B.), and Department of Crop Sciences (H.J.B.), University of Illinois, Urbana, Illinois 61801; Division of Applied Life Science, Gyeongsang National University, Jinju, Korea 660-701 (D.-H.O., H.H., R.A.B., D.-J.Y., H.J.B.); Department of Horticulture and Landscape Architecture, Purdue University, West Lafayette, Indiana 47907 (M.P.D., G.I., R.A.B., D.-J.Y.); Center for Plant Stress Genomics and Biotechnology, King Abdullah University of Science and Technology, Jeddah, Saudi Arabia 21534 (S.A., R.A.B., J.-K.Z., H.J.B.); Department of Plant Sciences and BIO5 Institute, University of Arizona, Tucson, Arizona 85721 (G.M.L., D.W.G.); and Department of Botany and Plant Sciences, University of California, Riverside, California 92521 (J.-K.Z.)

The genome of *Thellungiella parvula*, a halophytic relative of *Arabidopsis* (*Arabidopsis thaliana*), is being assembled using Roche-454 sequencing. Analyses of a 10-Mb scaffold revealed synteny with *Arabidopsis*, with recombination and inversion and an uneven distribution of repeat sequences. *T. parvula* genome structure and DNA sequences were compared with orthologous regions from *Arabidopsis* and publicly available bacterial artificial chromosome sequences from *Thellungiella salsuginea* (previously *Thellungiella halophila*). The three-way comparison of sequences, from one abiotic stress-sensitive species and two tolerant species, revealed extensive sequence conservation and microcolinearity, but grouping *Thellungiella* species separately from *Arabidopsis*. However, the *T. parvula* segments are distinguished from their *T. salsuginea* counterparts by a pronounced paucity of repeat sequences, resulting in a 30% shorter DNA segment with essentially the same gene content in *T. parvula*. Among the genes is SALT OVERLY SENSITIVE1 (*SOS1*), a sodium/proton antiporter, which represents an essential component of plant salinity stress tolerance. Although the *SOS1* coding region is highly conserved among all three species, the promoter regions show conservation only between the two *Thellungiella* species. Comparative transcript analyses revealed higher levels of basal as well as salt-induced *SOS1* expression in both *Thellungiella* species as compared with *Arabidopsis*. The *Thellungiella* species and other halophytes share conserved pyrimidine-rich 5' untranslated region proximal regions of *SOS1* that are missing in *Arabidopsis*. Completion of the genome structure of *T. parvula* is expected to highlight distinctive genetic elements underlying the extremophile lifestyle of this species.

The crucifer genus *Thellungiella* includes a number of species that have recently been recognized as models for identifying processes, pathways, and genes

of importance in plant abiotic stress tolerance (Bressan et al., 2001; Xiong and Zhu, 2002; Taji et al., 2004; Amtmann et al., 2005; Griffith et al., 2007). In particular, *Thellungiella salsuginea*, previously known as *Thellungiella halophila* (Al-Shehbaz and O'Kane, 1995; Amtmann, 2009), has been studied for its extreme salt, cold, and freezing tolerance and for its efficient mobilization of resources in poor or degraded soils (Kant et al., 2008). Another species, *Thellungiella parvula*, has been reported to have slightly higher salt and drought tolerance, being otherwise comparable to *T. salsuginea* in cold and freezing response characteristics (Orsini et al., 2010). The stress tolerance behavior of both species is appropriate to their natural habitats: of the several *T. salsuginea* ecotypes that have been collected, all are from stress-prone locations, such as the delta of the Yellow River in China, the Yukon Territory of

¹ This work was supported by King Abdullah University for Science and Technology of Saudi Arabia, by the World Class University Program, Korea (grant no. R32-10148), by the Biogreen 21 Project of the Rural Development Administration, Korea (grant no. 20070301034030), and by University of Illinois at Urbana-Champaign institutional support.

² These authors contributed equally to the article.

* Corresponding author; e-mail ohdongha@life.illinois.edu.

The author responsible for distribution of materials integral to the findings presented in this article in accordance with the policy described in the Instructions for Authors (www.plantphysiol.org) is: Dong-Ha Oh (ohdongha@life.illinois.edu).

^[W] The online version of this article contains Web-only data.

www.plantphysiol.org/cgi/doi/10.1104/pp.110.163923

Canada, and the Rocky Mountains of the United States. Similarly, the *T. parvula* ecotype used in this study originated from a salt flat in central Anatolia, Turkey.

Because of their close phylogenetic relationships to *Arabidopsis* (*Arabidopsis thaliana*; O'Kane and Al-Shehbaz, 2003) and because many transcripts have nucleotide sequence identities with the better known model in the 90% range (Wang et al., 2004; Taji et al., 2008), focusing on *Thellungiella* spp. in order to derive a molecular-level understanding of adaptation to challenging environments appears particularly appropriate. Both *Thellungiella* species are comparable to *Arabidopsis* in terms of growth rates and size under similar growth conditions and in terms of fertility, seed number, and ease of transformation by flower dipping (Inan et al., 2004).

A number of tools for comparative molecular characterizations have been developed for *T. salsuginea*, including tagged mutants, EST collections, and full-length cDNA collections (Inan et al., 2004; Taji et al., 2004, 2008; Wang et al., 2004, 2006; Gong et al., 2005; Wong et al., 2005). To date, results of stress challenge studies have identified transcriptome responses that are broadly similar to those shown by *Arabidopsis*. Some universally stress-responsive genes, however, appear to be highly expressed in *Thellungiella* even in the absence of challenges. Others are induced only at much higher levels of stress than their isologs in *Arabidopsis*. In addition, altered gene expression patterns appear to be more specific to the stress that is experienced. This contrasts with transcriptional responses in *Arabidopsis*, which are much less discriminating and typically are global (Gong et al., 2005; Kant et al., 2006).

In *Arabidopsis*, salt tolerance, albeit weak, is based on the action of a complex of two proteins (SALT OVERLY SENSITIVE3 [SOS3], a sensor, and SOS2, a protein kinase) involved in sensing and responding to the influx of sodium ions. This complex activates a number of proteins (Halfter et al., 2000; Cheng et al., 2004; Quan et al., 2007; Lin et al., 2009), including SOS1, a plasma membrane-located sodium/proton antiporter. Activation of SOS1 mediates the export of the Na⁺ ions, which may also be redistributed throughout the plant (Qiu et al., 2002; Quintero et al., 2002; Shi et al., 2002, 2003). The SOS complex exists in many other species, including *T. salsuginea*, suggesting that it is a general feature of plants. Recently, the importance of SOS1 in stress tolerance in *T. salsuginea* has been established using RNA interference to generate lines with reduced SOS1 transcript and protein abundances. These lines showed salt sensitivity nearly as pronounced as that exhibited by *Arabidopsis* (Oh et al., 2009).

Like *Arabidopsis*, both *T. parvula* and *T. salsuginea* have relatively small genomes. The *Thellungiella* species have seven pairs of chromosomes (Orsini et al., 2010). For *T. salsuginea*, the diploid genome size is about twice that of *Arabidopsis*, approximately 260

Mb (Inan et al., 2004). We now estimate, based on flow cytometry, a diploid genome size of approximately 180 Mb for *T. parvula*. These values, in combination with the *Arabidopsis* reference genome structure against which sequences can be compared, make genomic sequence analysis approachable.

Here, we report on our initial analyses of the *T. parvula* genome structure based on sequencing using the Roche-454 platform. Our objectives were to shed light on differences in the overall gene structure and composition of the *T. parvula* genome in comparison with those of *Arabidopsis* and *T. salsuginea*. We compare regions in the *T. parvula* genome with two bacterial artificial chromosome (BAC) sequences from orthologous regions in *T. salsuginea* (Deng et al., 2009; Nah et al., 2009) as well as with orthologous segments in the *Arabidopsis* genome and, in a three-species comparison, analyze gene and genome structures. We include an analysis of promoter structures, the presence and organization of repeats, and transcript expression for one of the genes in this region, *SOS1*, in an attempt to distinguish characteristics of the glycolytic and halophytic versions of this important salt tolerance determinant.

RESULTS

T. parvula genome sequences were determined by scaffold generating de novo assemblies constructed with Roche-454 GS-FLX Titanium single and paired-end sequencing. The average read lengths were 360 bp or greater in each paired-end library sequenced, a significant improvement compared with the predecessor version GS-FLX. Further sequencing and a draft genome assembly are in progress. We deduced a minimal genome size of 163.6 Mb, based on the total length of the preliminary assembly contigs. An independent estimate to the genome size of about 180 Mb was obtained through flow cytometric analysis of propidium iodide-stained nuclei (Supplemental Fig. S1).

Overview of *T. parvula* Genome Assembly and Analyses of a Scaffold

Table I summarizes the statistics of a genome draft assembly. The single end sequence assembly by Newbler and cleanup gave some 21,000 pieces that contain 163.6 Mb of contig sequences, which constitutes the minimal predicted genome size of *T. parvula*. Addition of paired-end libraries further assembled the contigs into 3,149 scaffolds encompassing 153.7 million bases. The scaffolds contain gaps, and incorporation of the reads from Illumina sequencing with higher coverage is in progress to fill in the gaps. Upon completion, the genome sequence will be released to the public.

One of the larger scaffolds (scaffold 00254) of 10,011,287 bp was subjected to further analysis. Scaffold 00254 had a GC content of 35.79%, comparable to

Table 1. Assembly statistics of the draft genome preliminary assembly

Criteria	Values
Total no. of reads used	24.89 million
Total no. of bases	5.9 Gb
Average read size	360 bp
No. of reads aligned to contigs	15.99 million (64%)
No. of reads excluded from the assembly as repeats	6.73 million
No. of paired end reads	7.16 million
Amount of both pairs mapped with correct orientation	60%
Amount of bases Q40 or greater	99.12%
Expected coverage	22×
No. of contigs	21,619
Total length of contigs	163.6 million bp
No. of contigs at least N50	1,316
Contig N50	31,906 bp
Minimum contig length	100 bp
Maximum contig length	600,277 bp
Median contig length	1,452 bp
Mean contig length	7,648 bp
No. of scaffolds	3,149
No. of scaffolds at least N50	10
Minimum scaffold length	900 bp
Maximum scaffold length	13,601,491 bp
Median scaffold length	3,660 bp
Mean scaffold length	48,828 bp
Scaffold N50	3,006,489 bp
Scaffold N90	28,644 bp
Total length of scaffolds	153.7 million bp
No. of Ns in the scaffolds	21,969

that of the Arabidopsis genome (36%). It had 346 gaps, with a mean predicted gap size of 757 bp, comprising 5.43% of the scaffold sequence. The scaffold contained overall 1.9% of repetitive sequences, including simple repeats, transposons, and retrotransposons, predicted by RepeatMasker. The distribution of repetitive sequences was not homogeneous, with the repeat contents usually very low at less than 0.5% over most of the sequences and dramatically increasing up to 15% toward the end of the scaffold sequence (Supplemental Fig. S2A). An ab initio open reading frame (ORF) prediction with FGENESH (<http://linux1.softberry.com/berry.phtml>) identified 2,229 ORFs, whose distribution showed a pattern opposite to the distribution of the repetitive sequences (Supplemental Fig. S2B). All 2,229 ORFs showed homology with an Arabidopsis gene locus at least for part of their sequences when subjected to BLASTn search against the Arabidopsis reference mRNA database (Supplemental Fig. S2C). When ORFs with total identity higher than 70% with Arabidopsis were considered, 73%, 15%, and 10% of the total predicted ORFs in scaffold 00254 showed the highest similarity with an Arabidopsis gene in chromosome 5, 3, and 2, respectively. To visualize the synteny between scaffold 00254 and Arabidopsis chromosomes, we provide a Circos plot linking the locations of the homologous ORFs between Arabidopsis and *T. parvula*. Scaffold 00254 showed extensive synteny with parts of Arabidopsis chromosomes 2, 3, and

5, with several rearrangement and inversion events, especially in the region showing colinearity with Arabidopsis chromosome 5 (Fig. 1).

T. parvula* Sequences Compared with Arabidopsis and *T. salsuginea

Scaffold 00254 contained regions orthologous to two recently published BAC sequences of *T. halophila* (now *T. salsuginea*; Deng et al., 2009; Nah et al., 2009). Here, we focus on these regions for a three-species comparison of genome sequences (Fig. 1, red bands on scaffold 00254). The gaps in the two focus regions were seamlessly filled with genomic PCR and Sanger sequencing with perfect matches in the adjacent sequences. Nah et al. (2009) isolated a *T. salsuginea* BAC sequence of 193.0 kb (termed here TS-1; National Center for Biotechnology Information [NCBI] GenBank accession no. FJ386403). The orthologous Arabidopsis genomic sequence is a 146.3-kb region (AT-1) located on chromosome 2. The corresponding genomic sequence in the *T. parvula* genome (TP-1; HM222924) is 134.3 kb in length. The second sequence analyzed here is orthologous to a randomly selected *T. salsuginea* BAC clone (82.9 kb; termed TS-2 here; DQ226510) presented by Deng et al. (2009). It is compared with a 79.3-kb DNA segment from Arabidopsis chromosome 5 and an orthologous 63.7-kb segment of *T. parvula*

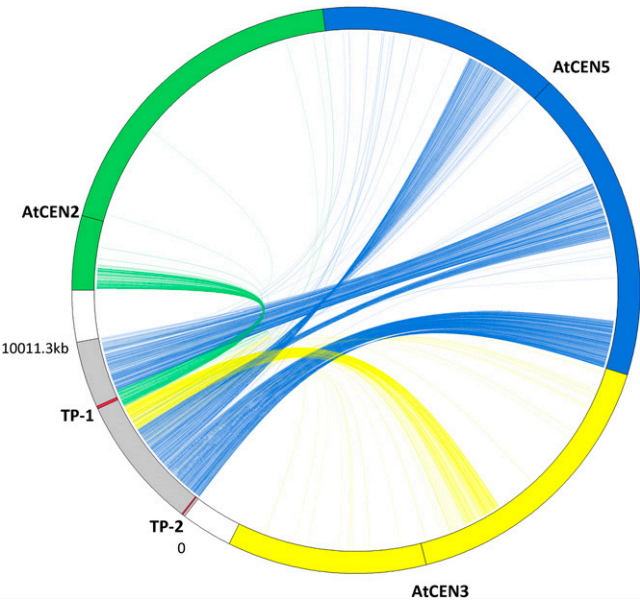


Figure 1. Synteny between a *T. parvula* scaffold and Arabidopsis chromosomes. A Circos plot depicting the *T. parvula* scaffold 00254 (gray) and Arabidopsis chromosomes 2 (green), 3 (yellow), and 5 (blue) is shown. The predicted *T. parvula* ORFs were connected to their putative Arabidopsis homologs, with the color of the connecting line designating the Arabidopsis chromosome, to visualize the synteny between two species. The two regions, TP-1 and TP-2, where the genomic sequences were available for three-species comparison are designated with red bands.

(TP-2; HM222925). Taken together, the overall G+C contents of the two regions in the *Thellungiella* species are slightly higher than those in *Arabidopsis*: 35.65% (*Arabidopsis*), 37.6% (*T. salsuginea*), and 36.3% (*T. parvula*).

Both regions for the three species were visualized using dot-plot alignments (Supplemental Fig. S3). The comparison identifies extensive colinearity between the species, with the highest degree between the two *Thellungiella* species. Several local rearrangements and deletions are obvious, indicated by boxes in Supplemental Figure S3, A and B, for the TP-1 region with respect to the AT-1 and TS-1 regions. In comparison with AT-2, TP-2 showed a large sequence inversion (Supplemental Fig. S3C). In contrast, TP-2 and TS-2 showed colinearity, with several expansions in TS-2 relative to the more compact TP-2 (Supplemental Fig. S3D).

Annotation of *T. parvula* Genes

The ORFs of the two *T. parvula* sequences were initially predicted ab initio using FGENESH. Homologous *Arabidopsis* and *T. salsuginea* genes were identified using BLASTx to the protein database of both species. Final ORF sequences were determined by FGENESH+ using the homologous *Arabidopsis* proteins as references. Supplemental Tables S1 and S2 list the predicted ORFs for TP-1 and TP-2, respectively, in comparison with the *Arabidopsis* and *T. salsuginea* sequences. ORFs for AT-1 and AT-2 were as annotated in TAIR9, and those for TS-1 and TS-2 as described by Nah et al. (2009) and Deng et al. (2009), respectively. The average gene densities are one per 5.17, 7.15, and 4.58 kb for TP-1, TS-1, and AT-1, respectively, and one per 2.89, 3.45, and 2.78 kb for TP-2, TS-2, and AT-2, respectively.

K_a/K_s (the ratio of the rate of nonsynonymous substitutions [K_a] to the rate of synonymous substitutions [K_s]) between the orthologous genes of three species were calculated, excluding genes of ambiguous orthology (Supplemental Table S3). For the two regions, 11 and 12 sets of genes, respectively, were analyzed. All gene pairs showed K_a/K_s ratios smaller than 1, indicating evolutionary selectivity among the orthologs favoring functional conservation. In all gene pairs, estimated divergences were older when comparing *Arabidopsis* with the two *Thellungiella* species than between *T. parvula* and *T. salsuginea*, averaging 12.3 million years ago between *T. parvula* and *Arabidopsis* and 12.4 million years ago between *T. salsuginea* and *Arabidopsis* but only 8.5 million years ago between *T. parvula* and *T. salsuginea* (Supplemental Table S3).

Synteny and Similarity

A graphical representation of the three-way comparison of distribution and spacing of genes in the two regions is given in Figure 2. TP-1 showed linear

similarity in the arrangement of the genes with both AT-1 and TS-1 (Fig. 2A). One conspicuous difference was the absence of transposons in TP-1 that were present in AT-1 and TS-1; the putative deletion sites are indicated with black arrows in Figure 2A. Both TP-1 and TS-1 contained longer intergenic regions between the genes encoding *SOS1* and their associated 5' gene models compared with AT-1 (Fig. 2A, red arrows). Orthologs of At_c (*TET14/AT2G01960*) were missing in both TP-1 and TS-1 (Fig. 2A, red box; Supplemental Table S1). In parts of the sequence, however, TP-1 showed higher similarity with AT-1 than with TS-1. For example, orthologous gene pairs Tp05/At_b (*AT2G01920*) and Tp18/At_d (*AT2G02061*) are absent in TS-1, while Th_A and Th_B, similar to AT1G14610 and AT2G02030, respectively, were not found in either TP-1 or AT-1 (Supplemental Table S1). TP-2 showed similarity in gene order with TS-2 (Fig. 2B), but both TP-2 and TS-2 showed an inversion of genes relative to AT-2 in part of the sequences. The break point for the inversion was at the position of At15 (*AT5G66410*; Fig. 2B, red arrow; Supplemental Table S2). In both *Thellungiella* species, sequence fragments with homologies to AT5G66410 were identified at the break point of the inversion. A gene homologous to AT5G66410, however, could not be identified in the entire *T. parvula* genome sequence (M. Dassanayake and D.-H. Oh, unpublished data).

Supplemental Figure S4 presents a detailed analysis of exon/intron structures and the overall sequence similarities. In comparing TP-1 and TP-2 with corresponding *Arabidopsis* and *T. salsuginea* sequences, the plot identified all exons of the orthologous genes; levels of identities were usually higher than 70%. Short stretches of sequence with significant (greater than 75%) identities were also present in intergenic regions, possibly designating regulatory elements or noncoding RNAs. However, we could not identify any tRNA, microRNA genes, or known small interfering RNA loci in the intergenic regions in any of the three species compared here.

In TP-1, several intergenic regions lacked homology with either *Arabidopsis* or *T. salsuginea* [Supplemental Fig. S4A, denoted (a)–(c)]. These discontinuities appear to be based either on a disruption of synteny by the insertion or deletion of genes (a) or transposable element insertion (b). The discontinuity in (c), however, is not explained. The intergenic region upstream of *TpSOS1* (TP1-10) was particularly interesting as it revealed homology with *T. salsuginea* but not with *Arabidopsis* (Supplemental Fig. S4A, dashed box). In contrast, differences in the intergenic regions between TP-2 and AT-2 involved translocations in TP-2 of genes whose *Arabidopsis* orthologs were from chromosomes other than chromosome 5: TP2-5, -7, and -16 are orthologs of AT3G53210, AT1G77370, and AT3G47840, respectively [Supplemental Fig. 4B, denoted (a)]. TP2-16 showed similarity with the AT-2 sequence for the latter half of the exons (Supplemental Fig. 4B, dashed box), which had also been observed in

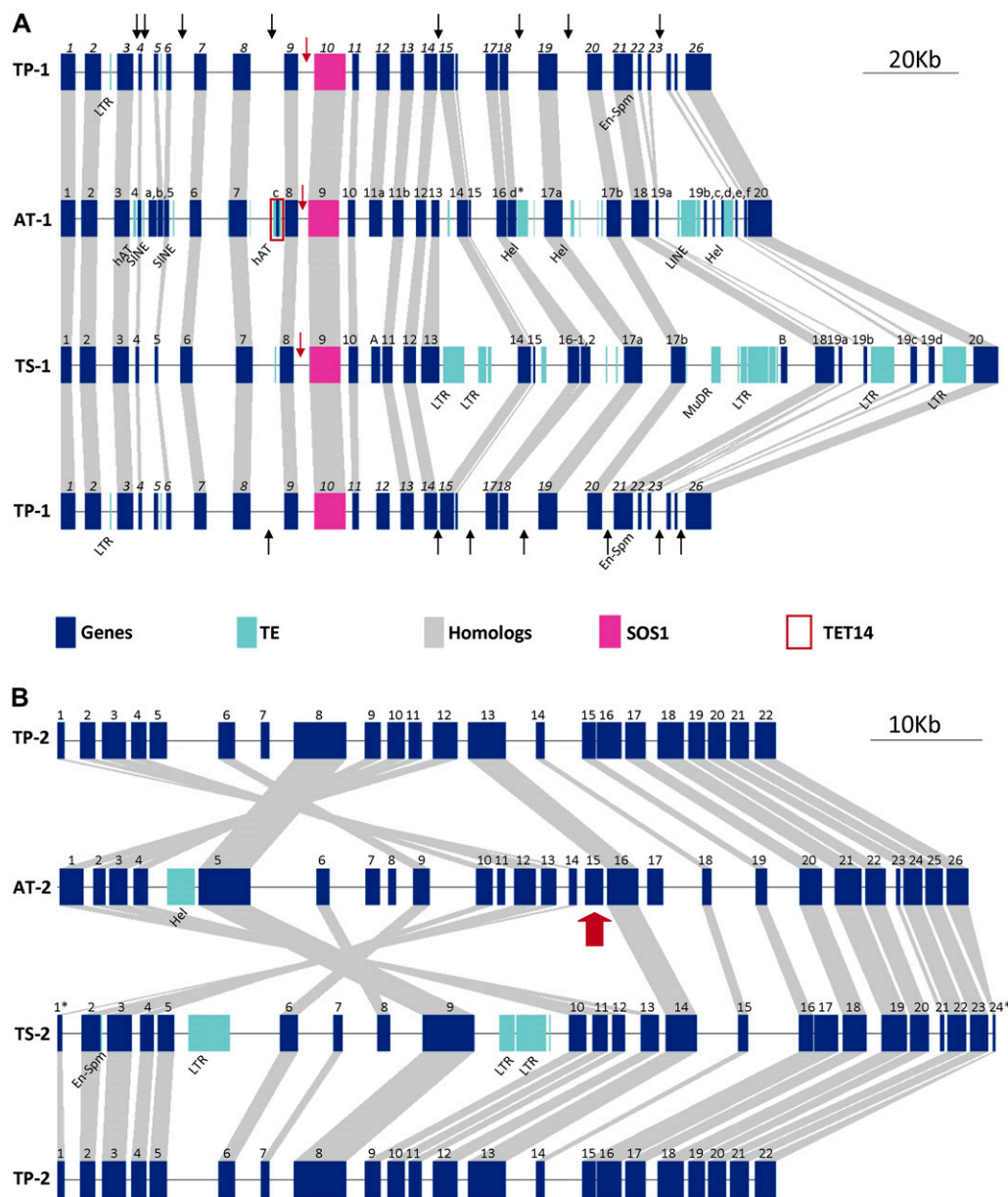


Figure 2. Genome organization for TP-1 (A) and TP-2 (B) in comparison with the organization of orthologous regions in Arabidopsis and *T. salsuginea*. A, Black arrows in TP-1 show deletions in comparison with AT-1 or TS-1. Red arrows indicate the intergenic space between SOS1 orthologs and their nearest 5' gene model. B, The inversion break point is indicated by a red arrow. Symbols for the genes are as in Supplemental Tables S1 and S2. Symbols used for transposable elements (TEs) are LTR (retrotransposon with long terminal repeats), SINE (short interspersed transposable elements), LINE (long interspersed transposable elements), MuDR (Mutator-like DNA transposon), Hel (helitron), En-Spm (Enhancer-Suppressor/Mutator transposon), and hAT (hAT family DNA transposon).

the comparison of TS-2 and AT-2 sequences (Deng et al., 2009).

Paucity of Repetitive Sequences in *T. parvula*

The three species show significant differences in repeat composition and frequency. Repeats in the form of transposable elements, however, are underrepresented (Fig. 2A) to absent (Fig. 2B) in *T. parvula*

compared with the other two species. In both TP-1 and TP-2, analyses using RepeatMasker and searches using other databases failed to identify a complete transposable element, while corresponding *T. salsuginea* and Arabidopsis sequences contained various retrotransposons and/or DNA transposable elements. In total, these elements span 17.6% (TS-1), 13.5% (TS-2), 8.7% (AT-1), and 3.0% (AT-2) of the sequences (Deng et al., 2009; Nah et al., 2009). In TP-1, small stretches of

sequences, less than 100 bp, suggested similarity with Arabidopsis transposable elements (Fig. 2A); such sequences amounted to less than 0.4% of the total length. TP-2 does not present even suggestions of transposable elements (Fig. 2B).

The paucity of repeats in *T. parvula* is less apparent, however, when tandem repeats are considered (Table II). As observed with transposable elements, sequence 2 has fewer tandem repeats than sequence 1 in all three species. Among the short tandem repeats, the dinucleotide AT_n is found at a much higher frequency than other dinucleotide, mononucleotide, trinucleotide, and tetranucleotide repeats in all three species. A survey of short tandem repeats in plants reported AT_n as the most abundant short tandem repeat in plant nuclear sequences (Wang et al., 1994).

Comparison of *SOS1* Genes

SOS1 was originally identified in Arabidopsis as an important element in the salinity stress tolerance pathway (Shi et al., 2000). Figure 3 presents a comparison of the *SOS1* promoters and coding regions in the two *Thellungiella* species and Arabidopsis. Homology between the promoter regions of *AtSOS1*, on the one hand, and *TpSOS1* or *TsSOS1*, on the other, was distinctly lacking (Fig. 3A), while PipMaker plots identified conserved motifs between the promoters of *TsSOS1* and *TpSOS1*. Although in the *SOS1* gene, *TpSOS1* showed higher identity with *TsSOS1* than with *AtSOS1* in general, different regions exhibited different levels of similarity. For example, *TsSOS1* showed higher similarity to *TpSOS1* in the N-terminal regions (Fig. 3B, exons 1–15), while *AtSOS1* and *TsSOS1* showed similar levels of similarity to *TpSOS1* in the C-terminal regions (Fig. 3B, exons 17–22).

Comparative Analyses of Transcription

Comparison of *SOS1* expression by reverse transcription (RT)-PCR previously revealed higher *SOS1* mRNA levels in *T. parvula* than in Arabidopsis under both normal and high-salt conditions, while house-keeping genes were expressed at similar levels in both species (Oh et al., 2009). Here, we compared the expression patterns of genes surrounding *SOS1* in the genome with that of *SOS1*, using quantitative real-time RT-PCR (Fig. 4; Supplemental Table S4). *SOS1* showed 2.6- and 1.5-fold higher mRNA levels in *T. parvula* shoot and root tissues, respectively, than in Arabidopsis in the absence of stress. Salt stress in-

duced *SOS1* expression up to 9.5- and 4.7-fold higher in *T. parvula* shoots and roots, respectively, while induction was only 1.59- and 2.3-fold in Arabidopsis shoots and roots (Supplemental Table S4). Similar increases in *T. parvula* were found also after the addition of 350 mM NaCl, a concentration lethal for Arabidopsis ecotype Columbia. The higher *SOS1* level in *T. parvula* compared with Arabidopsis is similar to the previous observation for *SOS1* in *T. salsuginea* (Oh et al., 2009). For other genes tested in the vicinity of *SOS1*, differences in gene expression between the species were less dramatic (Fig. 4B; Supplemental Table S4).

Also included in the real-time PCR analyses (Fig. 5) were three genes not located on Arabidopsis chromosome 5 but found in TP-2 as genes that disrupted the colinear order of genes: AT3G53210, AT1G77370, and AT3G47840. Analysis was extended to the AT5G66460 ortholog adjacent to AT3G47840 and induced by abscisic acid and salt stress (Zimmermann et al., 2004). The AT3G53210, AT1G77370, and AT3G47840 orthologs were found as single-copy genes in the *T. parvula* genome sequenced by a combination of Roche-454 and Illumina/Solexa sequencing, which is at present in the final assembly phase (M. Dassanayake and D.-H. Oh, unpublished data). As expected, quantitative real-time RT-PCR amplified single species of amplicons using *T. parvula* cDNA for all three genes. The most dramatic difference in expression between Arabidopsis and *T. parvula* was observed with AT3G53210, annotated as encoding a nodulin family protein, in which the mRNA was significantly higher in the shoots of *T. parvula* than in Arabidopsis, and was further induced by salt stress. AT1G77370 showed generally higher mRNA abundance in *T. parvula* under all conditions, while the AT5G66460 basal expression was at a lower level, in both shoot and root, than in Arabidopsis. Expression of the AT3G47840 ortholog did not show significant differences between *T. parvula* and Arabidopsis (Fig. 5; Supplemental Table S4).

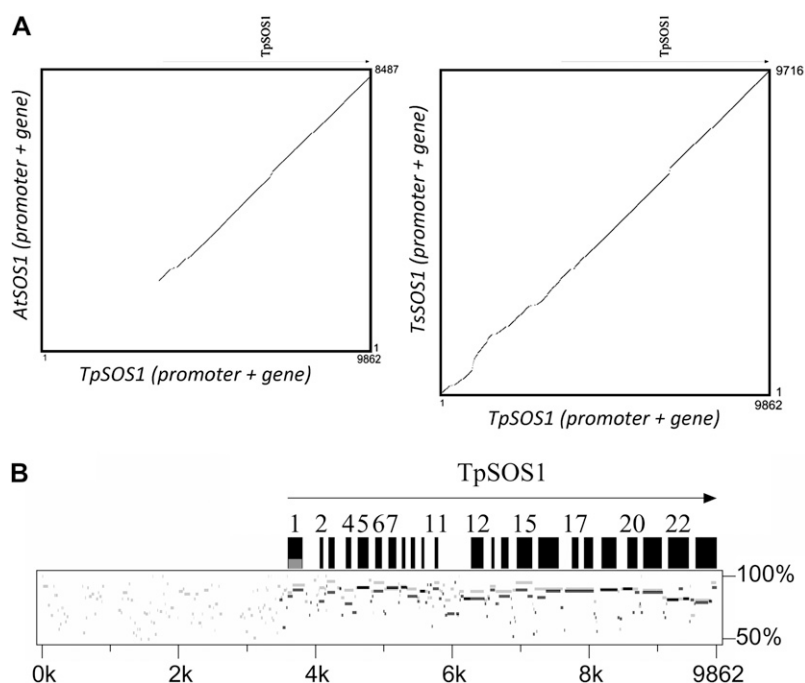
Analyses of Sequences Upstream of *SOS1*

Although functions and domains of *SOS1* genes have been extensively studied in a few species, little is known about transcriptional regulation and promoter evolution in this gene family. In the three species, searches for cis-elements in the region up to 2,000 bp upstream from the *SOS1* translation start site (predicted for *T. parvula*) identified several known stress-responsive elements. These included abscisic

Table II. Tandem repeat distribution in the three species

Variable	TP-1	AT-1	TS-1	TP-2	AT-2	TS-2
No. of bases in tandem repeats	1,661	1,747	2,521	417	1,056	847
No. of tandem repeat loci	26	28	49	7	11	10
No. of short tandem repeat loci	10	8	10	1	2	4
No. of long tandem repeat loci	16	20	39	6	9	6

Figure 3. Comparison of the SOS1 homologs in *T. parvula*, *T. salsuginea*, and Arabidopsis. The genomic sequence spanning the 5' intergenic space and SOS1 genes from *T. parvula* was compared with the corresponding regions in *T. salsuginea* and Arabidopsis using dot plot (A) and PipMaker plot (B). In B, the PipMaker plots comparing *TpSOS1* with *TsSOS1* (gray) and *AtSOS1* (black) were superimposed to show the differences in similarity. Word size of the PipMaker plot was 7 bp.



acid-response elements, anaerobic induction elements, a MYB-binding site involved in drought inducibility, heat stress-responsive elements, low temperature-responsive elements, and defense- and generally stress- and hormone-responsive elements (Supplemental Table S5).

A comparison of *SOS1* transcript structures of halophytes and glycophytic species revealed a surprising difference between the two groups. When analyzing the 5' untranslated regions (UTRs) of *SOS1* genes, we found differences in CT content of a stretch extending 100 bp immediately upstream of the translation start sites of all available genes in the NCBI nucleotide databases and the published plant genomes available on Phytozome (<http://www.phytozome.net>). The highest pyrimidine ratio was found in the two *Thellungiella* species, and the largest difference between two species in the list separated *Salicornia*, a halophyte, from *Manihot*, a glycophyte (Fig. 6). Within the *SOS1* 5' UTR adjacent to the translation start site, there are 12 and 18 CTT repeats in *T. parvula* and *T. salsuginea*, respectively. The Arabidopsis sequence shows three CTT repeats in the homologous region. In addition, these CT-rich sequences are associated with a region that could potentially form stem-loop structures in proximity to the initiation ATG codon (Supplemental Fig. S5).

DISCUSSION

Abiotic stress tolerance and sensitivity are unequally distributed among plant species. Although most species are stress sensitive, there are, interestingly, also stress-tolerant species in most families.

Moreover, there is significant plasticity in environmental adaptation; even many species that are typically viewed as stress sensitive have salt-tolerant ecotypes. Thus, it seems highly likely that the basic machinery for adaptation to a stressful environment is universally endowed in plant genomes. It is unclear, however, whether the potential for adaptation has failed to develop in some environments or whether it has secondarily been lost in less demanding environments or through human invention. Given the importance of fresh water for agriculture and the increasing salinization of many irrigated lands, especially in dry, subtropical areas, it is important that we find the signposts indicating salinity stress tolerance and that we know about the essential processes and genes (Cheeseman, 1988; Hasegawa et al., 2000; Zhu, 2001; Flowers, 2004; Flowers and Colmer, 2008).

In this paper, we address these goals using high-throughput sequencing. Our strategy was to employ closely related plant species that exhibit very different salt stress tolerance characteristics. Although genome sequencing by Joint Genome Initiative is reported to have been completed, the available genomic resources for *T. salsuginea* are still limited. We have concentrated on two BAC clones for *T. salsuginea* (Deng et al., 2009; Nah et al., 2009) and the orthologous regions in Arabidopsis and *T. parvula*. A three-way comparison revealed similarities in the synteny and gene structures among the two genome segments. Synteny, as expected, is more pronounced among the *Thellungiella* species. Orthologous genes showed functional conservation, as supported by the K_a/K_s values. However, there were differences in genome features and sequences between the *Thellungiella* species and

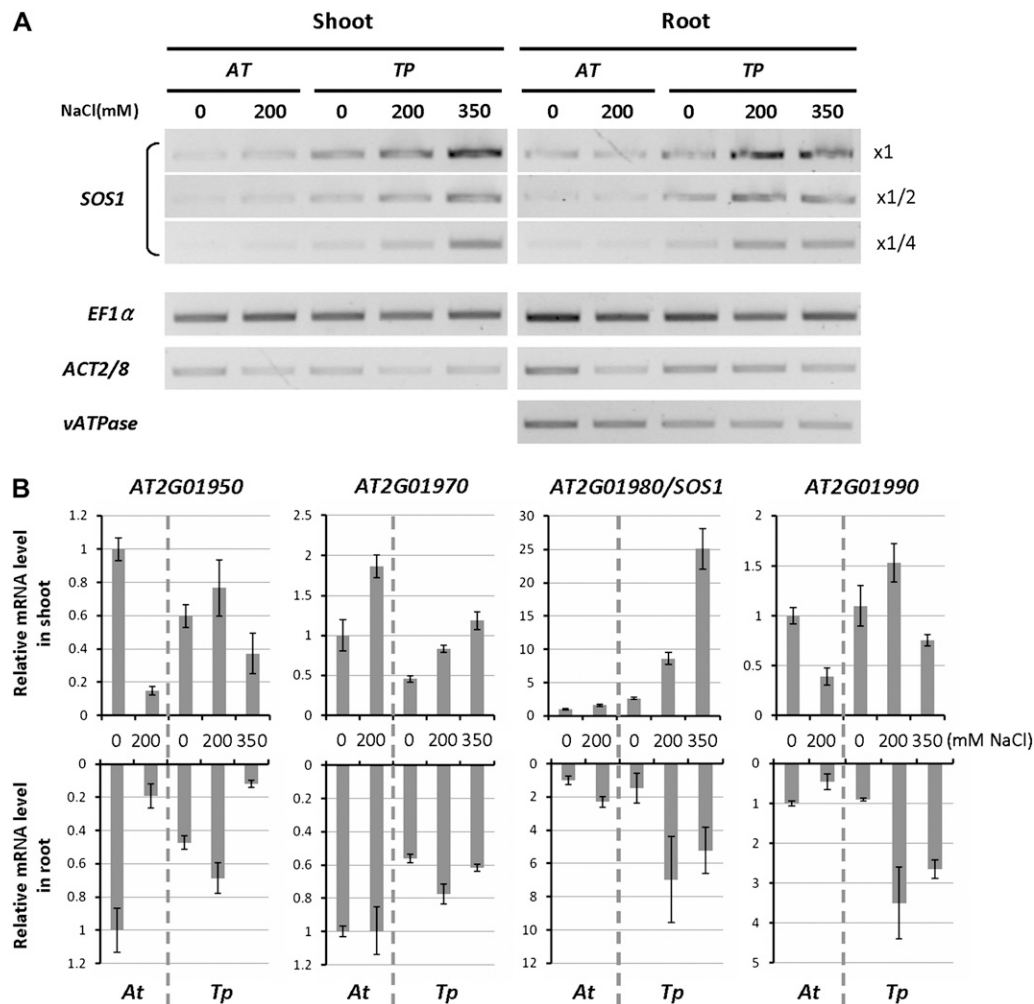


Figure 4. Analysis of *SOS1* mRNA abundance in *Arabidopsis* and *T. parvula* *SOS1*. *SOS1* mRNA levels were compared between *Arabidopsis* and *T. parvula* with RT-PCR (A) and quantitative real-time PCR (B). In A, dilution series of cDNA were used for *SOS1* to ensure that the reaction was performed in a linear range. In B, relative mRNA levels were normalized with *EF1α* as a reference. Fold differences compared with the nonstressed *Arabidopsis* sample are shown. Error bars indicate the SD from six repeats (two biological and three analytical repeats). Expression patterns of orthologous genes around *SOS1* are shown for comparison.

Arabidopsis and also within the *Thellungiella* genus. Some of these may be expected to be related to physiological differences that separate the three species.

Differences between the *Thellungiella* Species and *Arabidopsis*

Based on the K_s values of orthologous genes, the divergence of *T. parvula* and *T. salsuginea* from *Arabidopsis* can be placed at approximately 12 million years ago, and the *Thellungiella* species separated approximately 8 million years ago. The observed genome structures, inversions, and breaks in the colinearity are consistent with the time of divergence.

An obvious difference with respect to *Arabidopsis* and a specific feature of the *Thellungiella* species identified genome sequences around the *SOS1* gene, one of

the well-established salt tolerance determinants (Shi et al., 2000). Irrespective of extensive synteny of the ORFs and the conservation of gene structures for *SOS1* between *Arabidopsis* and *T. parvula*, colinearity falls apart starting upstream of the first exon in *SOS1* (Fig. 3). A hypothesis based on the analysis of *SOS1* expression in *T. salsuginea* (Oh et al., 2009) suggested different expression strength or, possibly, transcript stability. This is further supported in *T. parvula* by the analysis of *SOS1* mRNA levels in comparison with *Arabidopsis* (Fig. 4). Coupled with the significant sequence similarity in the *SOS1* 5' UTR of halophytic species (Fig. 6), a closer examination of this transcript structural feature is appropriate because it may point to a fundamental glycophyte-halophyte distinguishing character that is less or not apparent when promoter cis-elements are compared. The hypothesis of a halophytic transcript structure is particularly attrac-

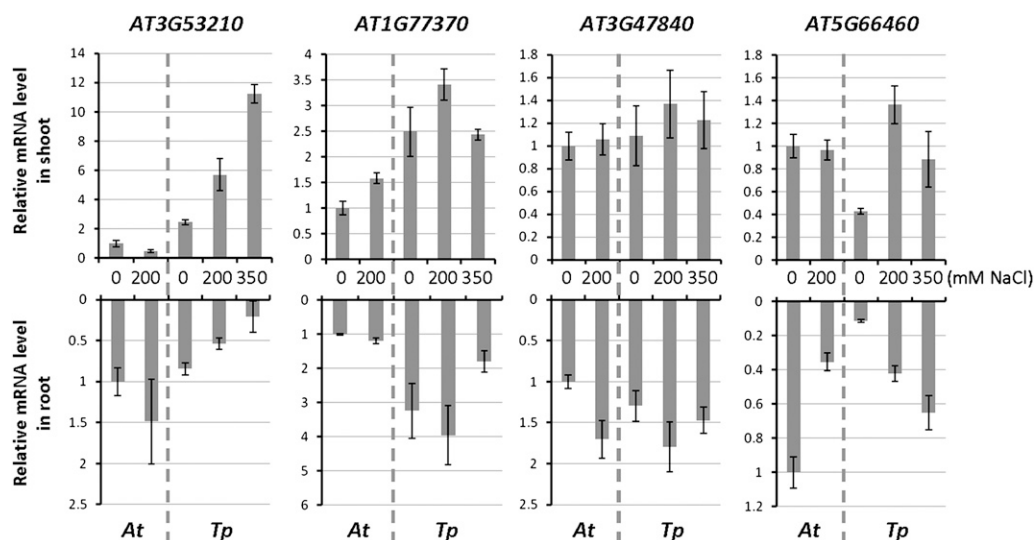


Figure 5. Comparison of gene expression of translocated genes in *T. parvula*. Shown are quantitative real-time PCR results comparing the expression of selected orthologous genes from TP-2. Normalization and error bars are as in Figure 4B.

tive because of the very similar pyrimidine tracts, CT_n, present in the promoters of *Chenopodium quinoa* and *Salicornia brachiata*, which are both recognized as halophytes (Sanchez et al., 2003; Lieth et al., 2008). The possibility of *TsSOS1* and *TpSOS1* 5' UTR sequences involved in the formation of hairpin structures with free energies of -4.0 and -5.40 kcal mol⁻¹, respectively, close to the protein initiation codon enforces the notion that this structure appears to be important (Supplemental Fig. S5). Very similar stem-loop structures also characterize the 5' UTR of the two other halophytes for which this sequence information is available.

Analyzing the conservation of (C_nT_n)_n repeats on the 5' UTR sequences in all stress-related and highly expressed genes is beyond the scope of this study. However, we investigated the emerging apparent pattern in genes with high expression levels or highly induced under abiotic stress in *Arabidopsis* and the two *Thellungiella* species. The availability of publicly available 5' UTR sequences from *T. salsuginea* full-length transcripts limited candidate genes to a small collection. Nevertheless, a general pattern appears to be preserved in highly expressed genes, and the prevalence of CT-rich regions is more prominent in the two *Thellungiella* species compared with *Arabidopsis*. *Arabidopsis* heat shock protein 70 (AT3G09440) is known to be highly expressed under abiotic stress, including salt stress, both in *Arabidopsis* and *T. salsuginea* (Taji et al., 2004; Swindell et al., 2007). There is a pyrimidine-rich region close to the ATG initiation codon in the putative homologs of *Thellungiella* 5' UTR sequences (Supplemental Fig. S6). Similar observations were found for cytosolic cyclophilin ROC3 (peptidyl-prolyl cis-trans isomerase; AT2G16600) and a transcription factor B3 (AT4G21550). Cyclophi-

lins such as ROC3 are highly abundant cytosolic proteins known to be induced under abiotic stress (Chou and Gasser, 1997; Romano et al., 2004), and in addition to broad-range stress-responsive expression, the transcription factor AT4G21550 is also induced in specific developmental stages (Suzuki et al., 2007). All nine 5' UTR sequences can form stem-loop structures close to the initiation codon.

Formation of this hairpin structure could affect transcription efficiency or the stability of the transcript, although this topic, while analyzed in the past in bacterial and viral systems (Simoes and Sarnow, 1991; Emory et al., 1992; Hellendoorn et al., 1997), has not received much attention in plants (Klaff et al., 1996). Pyrimidine-rich elements in the 5' UTR of plants are known to have positive effects on transcription (Bolle et al., 1994), and they appear to be functionally conserved in diverse gene families across the plant kingdom. A similar pyrimidine-rich element in the 5' UTR has been shown to confer high transcription levels without the need for other upstream cis-elements except for a TATA box in tomato (*Solanum lycopersicum*) hydroxy-3-methylglutaryl CoA reductase genes (Daraselia et al., 1996). Also, actin genes from *Arabidopsis* to *Physcomitrella* include 5' UTR pyrimidine-rich stretches, which have been associated with very high levels of transcription (An et al., 1996; An and Meagher, 2010).

Finally, the possibility exists that the CT_n sequence domains in halophyte species upstream of the ATG codon might be a target of DNA chromatin modifications that could exert additional expression control. Hypermethylation in *Arabidopsis* *SUPERMAN* and *AGAMOUS* genes is thought to be influenced through DNA secondary structures formed by pyrimidine-rich sequences (Jacobsen et al., 2000).

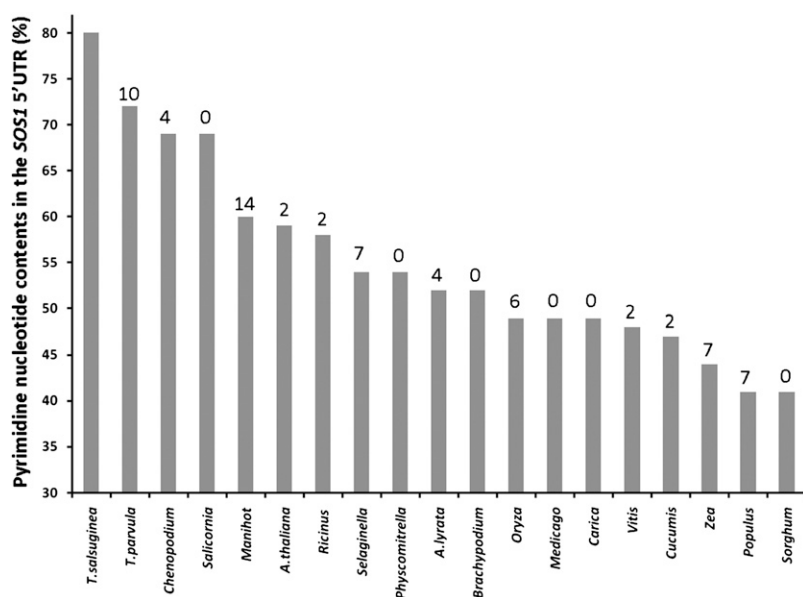


Figure 6. Frequency of pyrimidine nucleotides in SOS1 5' UTR sequences of diverse organisms. CT content values (%) are sorted from large to small, and the percentage difference between two consecutive columns is shown above each column. Additional sequences are *Chenopodium quinoa* (gi:154269387), *Salicornia brachiata* (gi:214028395), *Populus trichocarpa* gene POPTR_0010s11130, *Manihot esculenta* cassava39868.m1, *Ricinus communis* 29780.t000067, *Medicago truncatula* Medtr2g043140, *Cucumis sativus* Cucsa.026500, *Arabidopsis lyrata* SOS1, *Oryza sativa* LOC_Os12g44360, *Carica papaya* evm.TU.supercontig_2.63, *Vitis vinifera* gene GSVIVT00030673001, *Sorghum bicolor* Sb08g023290, *Zea mays* GRMZM2 G098494, *Brachypodium distachyon* Bradi4g00290, *Selaginella moellendorffii*, *Physcomitrella patens*, and *Chlamydomonas reinhardtii* Au9.Cre24.g769600. One hundred nucleotides upstream of the translation start site was taken unless a shorter 5' UTR was defined for a given species.

Differences between *T. parvula* and *T. salsuginea*

At approximately 180 Mb, the genome of *T. parvula* is significantly smaller than that of *T. salsuginea*, which is estimated as at least 260 Mb (Inan et al., 2004; Nah et al., 2009). The estimated genome based on a preliminary assembly permits us to assume approximately 163 Mb for *T. parvula* (Table I). Among the largest contributors to angiosperm genome size variations are repetitive DNAs and transposable elements (Ma et al., 2004; Meagher and Vassiliadis, 2005; Gaut and Ross-Ibarra, 2008). The comparison of orthologous genomic regions in this study between the two *Thellungiella* species showed *T. salsuginea* to be of consistently larger size, with the difference relating to the insertion of various transposable elements (Fig. 2). In contrast, the *T. parvula* genomic regions analyzed here showed a more compact gene organization than that seen in *Arabidopsis*, largely due to the absence of transposable elements and small repeat regions. If the prediction of a more compact structure is maintained across the entire genome, it is possible that *T. parvula* contains a higher total number of genes as compared with *Arabidopsis*. The lack of repetitive sequences extended to the bigger genomic region (scaffold 00254), with an overall repeat content as low as 1.9%. However, the *T. parvula* sequence also revealed regions rich in repetitive sequences; for example, the last 50-kb region of scaffold 00254 contained more than 15% repetitive sequences (Supplemental Fig. S2A), possibly indicating that this region was adjacent to a centromeric region in the corresponding *T. parvula* chromosome.

The genome size and complexity differences of the *Thellungiella* species can potentially provide explanations for their different growth habits and physiological trait differences. Differences include rosette formation in *T. salsuginea* but not in *T. parvula* and differences in stomatal conductance, stomata density,

and water loss (Orsini et al., 2010). Differences also include growth parameters, with *T. parvula* as a fast-growing species that is adapted to high light that shows etiolation under *Arabidopsis*-type light conditions. In contrast, *T. salsuginea* shows a much slower growth rate, possibly a reflection of its adaptation to typically resource-poor habitats (Inan et al., 2004; Gong et al., 2005; Oh et al., 2009).

Toward the *T. parvula* Genome Sequence

T. salsuginea (salt cress) has been studied as a model halophyte, juxtaposing its physiology and genetic structure to that of *Arabidopsis*. Suggested mechanisms for tolerance to stress and nutrient-limiting conditions include control over stomatal conductance (Inan et al., 2004), greater discriminatory power of K^+ - and Na^+ -transport systems (Volkov et al., 2004; Volkov and Amtmann, 2006), and nitrogen utilization efficiency (Kant et al., 2008). However, a genetic basis of the differences in tolerance could only be deduced by attempts at establishing *Arabidopsis*-like resources and databases (Inan et al., 2004; Taji et al., 2004, 2008; Wang et al., 2004, 2006; Gong et al., 2005; Wong et al., 2005; Zhang et al., 2008; Oh et al., 2009). Merging the forthcoming *T. parvula* genome sequence in a three-way comparison that includes *Arabidopsis* and *T. salsuginea* (pending; <http://www.jgi.doe.gov/sequencing/why/50029.html>) will provide a powerful way to probe for the essence of halophytism, in particular if other crucifer species and ecotypes of well-studied species are included (Weigel and Mott, 2009; Orsini et al., 2010).

Halophytism is an intriguing ecophysiological adaptation to saline environments. However, defining its essence in molecular or genetic terms has been elusive, due in a large part to the observation that many

different strategies have evolved by which species became tolerant or resistant to the stress. What appears to emerge is the existence of a small number of novel genes (Vinocur and Altman, 2005), while novel uses of kingdom-wide existing genes and proteins seem to provide the bulk of the mechanisms that form the basis of the stress-tolerance phenotype. Increasingly, halophyte transcriptomes are being analyzed and contrasted to glycophytic relatives (Kore-eda et al., 2004; Gong et al., 2005; Zouari et al., 2007; Dassanayake et al., 2009; Guo et al., 2009; Chelaifa et al., 2010). With the advent of numerous ongoing whole genome sequencing projects and comparisons throughout the plant kingdom, a multifaceted approach becomes possible. The result will be the integration of results on genome organization, gene and transcript structures, noncoding regulatory RNAs, regulatory mechanisms, biochemical complexity, and hormone- or metabolite-based signaling networks. From integration will emerge understanding of the processes that enabled individual species in all plant orders to use common genes in the evolution of a halophytic way of life.

MATERIALS AND METHODS

Plant Material

The ecotype of *Thellungiella parvula* used here was collected around a saline lake in the Tuz Golu region occupying a depression on the central plateau of Turkey at an elevation of 905 m above sea level. For most of the year, the shallow (1–2 m) saline lake covers an area of approximately 1,500 km². Water density is 1.225 g cm⁻³ (32.4% salt). The lake has no outlet; only a few surface streams feed into it, which may run dry in summer. During the summer months (with temperatures of greater than 40°C), the lake can evaporate completely. Precipitation in the area averages 250 mm per year. An inbred line was used for the genome sequencing and analyses.

Plant Growth and Genome Size

Genomic DNA was extracted from 10-d-old seedlings of *T. parvula* using the Genomic DNA Preparation Kit (Illumina). For gene expression analyses, total RNAs were isolated from 10-d-old seedlings of *T. parvula* and *Arabidopsis* (*Arabidopsis thaliana*) at the stage when the first true leaves emerge. Salt stress treatment and sample harvest were done as described by Oh et al. (2009). Genome size was determined by flow cytometry using a Becton-Dickinson LSR II (BD Biosciences). Homogenates of *Arabidopsis* and *T. parvula* were prepared by chopping leaves, and nuclei were stained with 40 µg mL⁻¹ propidium iodide (Galbraith et al., 1983). Samples were analyzed at an event rate of 200 nuclei s⁻¹. The configuration for propidium iodide detection comprised 488-nm laser excitation and a 630/22-nm band-pass filter. Chromosome numbers were determined in root tips after staining of mitotic cells (M. Dassanayake and D.-H. Oh, unpublished data).

DNA Libraries, DNA Sequencing, and Sequence Assembly

T. parvula DNA was isolated and prepared for Roche-454 GS FLX Titanium series long-read and paired-end sequencing and initial flowgram data processing following standard protocols (Roche-454 Life Sciences). Roche-454 sequences from eight single-ended genomic shotgun libraries and the respective titration plates were first assembled using Newbler (version 2.0.01.14) with a 40-bp minimum overlap and 90% identity. Sequences from one 2.5-kb, three 3-kb, two 8-kb, and one 20-kb paired-end libraries were added to the existing contigs to build scaffolds. A total of 24.89 million reads with a total of 5.9 Gb and an average read length of 360 bp were used for the de novo genome assembly with an inferred read error of 1.25%. A total of 99.2% of the bases

used had a quality score of Q40 or greater. The two *T. parvula* genomic regions corresponding to the two BAC clones of *Thellungiella salsuginea* were selected using BLASTn. The sequence gaps in these regions were filled by PCR with specific primers targeted to flanking regions of the gaps in the assembly. Sanger sequencing of genomic PCR products was used to fill sequencing gaps and to confirm the sequences adjacent to the gaps.

Sequence Analysis and Annotation

The ORFs in genomic sequences were predicted ab initio with FGENESH (<http://www.softberry.com>) adopting *Arabidopsis* parameters. The predicted ORFs were annotated using the NCBI nonredundant databases and the TAIR9 database (<http://www.arabidopsis.org/>) with BLASTn and BLASTP programs. When analyzing TP-1 and TP-2, the ORF predictions were refined using FGENESH+ with *Arabidopsis* orthologous proteins as references. Repeat elements were identified by RepeatMasker (<http://www.repeatmasker.org/cgi-bin/WEBRepeatMasker>) and the program Tandem Repeats Finder version 4.04 (Benson, 1999). The homologous sequence comparisons were made with PipMaker (Schwartz et al., 2000) and dot-plot analysis (Sonnhammer and Durbin, 1995).

Quantitative RT-PCR

Primers were designed to have identical sequences and amplifying amplicons of identical size from *T. parvula* and *Arabidopsis* cDNAs (Supplemental Table S6). Quantitative real-time RT-PCR was performed as described previously (Poroyko et al., 2007; Oh et al., 2010). For the reference genes, orthologs of EF1α (AT5G60390) and cytochrome *c* (AT5G40810) from the *T. parvula* transcriptome (M. Dassanayake and D.-H. Oh, unpublished data) were used and gave similar results. Represented in Figures 4 and 5 are results normalized to EF1α from six repeats (two biological and three analytical repeats).

Sequence data from this article can be found in the GenBank/EMBL data libraries under accession numbers HM222924 and HM222925.

Supplemental Data

The following materials are available in the online version of this article.

Supplemental Figure S1. Comparison of relative DNA contents by flow cytometry.

Supplemental Figure S2. Analysis of scaffold 00254.

Supplemental Figure S3. Comparison between *T. parvula* genomic sequences TP-1 and TP-2 with three orthologous genomic regions in *Arabidopsis* and *T. salsuginea*.

Supplemental Figure S4. Syntenic relationships and homologies of sequences represented by percent identity plots.

Supplemental Figure S5. Hairpin structures in the 5' UTR of the halophytic *Thellungiella* species.

Supplemental Figure S6. Comparison of CT tracts in the 5' UTRs of various genes among the three species.

Supplemental Table S1. ORFs identified in TP-1, AT-1, and TS-1.

Supplemental Table S2. ORFs identified in TP-2, AT-2, and TS-2.

Supplemental Table S3. Comparison of *K_a/K_s* ratios in orthologous genes and the estimated divergence time of three species.

Supplemental Table S4. Comparison of relative gene expression levels by quantitative PCR.

Supplemental Table S5. Known cis-elements in SOS1 promoter regions up to 2,000 bp upstream of the translation start site.

Supplemental Table S6. List of PCR primers.

ACKNOWLEDGMENTS

We thank Keith Frazier and Jyothi Thimmapuram (Keck Center for Comparative and Functional Genomics, University of Illinois at Urbana-Champaign) for advice and generous help.

Received August 3, 2010; accepted September 8, 2010; published September 10, 2010.

LITERATURE CITED

- Al-Shehbaz IA, O'Kane SL Jr (1995) Placement of *Arabidopsis parvula* in Thellungiella (Brassicaceae). *Novon* 5: 309–310
- Amtmann A (2009) Learning from evolution: Thellungiella generates new knowledge on essential and critical components of abiotic stress tolerance in plants. *Mol Plant* 2: 3–12
- Amtmann A, Bohnert HJ, Bressan RA (2005) Abiotic stress and plant genome evolution: search for new models. *Plant Physiol* 138: 127–130
- An Y, Meagher R (2010) Strong expression and conserved regulation of ACT2 in *Arabidopsis thaliana* and *Physcomitrella patens*. *Plant Mol Biol Rep* 28: 481–490
- An YQ, Huang S, McDowell JM, McKinney EC, Meagher RB (1996) Conserved expression of the *Arabidopsis* ACT1 and ACT3 actin subclass in organ primordia and mature pollen. *Plant Cell* 8: 15–30
- Benson G (1999) Tandem repeats finder: a program to analyze DNA sequences. *Nucleic Acids Res* 27: 573–580
- Bolle C, Sopory S, Lübberstedt T, Herrmann RG, Oelmüller R (1994) Segments encoding 5'-untranslated leaders of genes for thylakoid proteins contain cis-elements essential for transcription. *Plant J* 6: 513–523
- Bressan RA, Zhang C, Zhang H, Hasegawa PM, Bohnert HJ, Zhu JK (2001) Learning from the Arabidopsis experience: the next gene search paradigm. *Plant Physiol* 127: 1354–1360
- Cheeseman JM (1988) Mechanisms of salinity tolerance in plants. *Plant Physiol* 87: 547–550
- Chelaifa H, Mahé F, Ainouche M (2010) Transcriptome divergence between the hexaploid salt-marsh sister species *Spartina maritima* and *Spartina alterniflora* (Poaceae). *Mol Ecol* 19: 2050–2063
- Cheng NH, Pittman JK, Zhu JK, Hirschi KD (2004) The protein kinase SOS2 activates the Arabidopsis H⁺/Ca²⁺ antiporter CAX1 to integrate calcium transport and salt tolerance. *J Biol Chem* 279: 2922–2926
- Chou IT, Gasser CS (1997) Characterization of the cyclophilin gene family of Arabidopsis thaliana and phylogenetic analysis of known cyclophilin proteins. *Plant Mol Biol* 35: 873–892
- Daraselia ND, Tarchevskaya S, Narita JO (1996) The promoter for tomato 3-hydroxy-3-methylglutaryl coenzyme A reductase gene 2 has unusual regulatory elements that direct high-level expression. *Plant Physiol* 112: 727–733
- Dassanayake M, Haas JS, Bohnert HJ, Cheeseman JM (2009) Shedding light on an extremophile lifestyle through transcriptomics. *New Phytol* 183: 764–775
- Deng Z, Li Y, Xia R, Wang W, Huang X, Zhang L, Zhang S, Yang C, Zhang Y, Chen M, et al (2009) Structural analysis of 83-kb genomic DNA from *Thellungiella halophila*: sequence features and microcolinearity between salt cress and *Arabidopsis thaliana*. *Genomics* 94: 324–332
- Emory SA, Bouvet P, Belasco JG (1992) A 5'-terminal stem-loop structure can stabilize mRNA in *Escherichia coli*. *Genes Dev* 6: 135–148
- Flowers TJ (2004) Improving crop salt tolerance. *J Exp Bot* 55: 307–319
- Flowers TJ, Colmer TD (2008) Salinity tolerance in halophytes. *New Phytol* 179: 945–963
- Galbraith DW, Harkins KR, Maddox JM, Ayres NM, Sharma DP, Firoozabady E (1983) Rapid flow cytometric analysis of the cell cycle in intact plant tissues. *Science* 220: 1049–1051
- Gaut BS, Ross-Ibarra J (2008) Selection on major components of angiosperm genomes. *Science* 320: 484–486
- Gong Q, Li P, Ma S, Indu Rupassara S, Bohnert HJ (2005) Salinity stress adaptation competence in the extremophile *Thellungiella halophila* in comparison with its relative *Arabidopsis thaliana*. *Plant J* 44: 826–839
- Griffith M, Timonin M, Wong AC, Gray GR, Akhter SR, Saldanha M, Rogers MA, Weretilnyk EA, Moffatt B (2007) Thellungiella: an Arabidopsis-related model plant adapted to cold temperatures. *Plant Cell Environ* 30: 529–538
- Guo YQ, Tian ZY, Qin GY, Yan DL, Zhang J, Zhou WZ, Qin P (2009) Gene expression of halophyte *Kosteletzkya virginica* seedlings under salt stress at early stage. *Genetica* 137: 189–199
- Halfert U, Ishitani M, Zhu JK (2000) The Arabidopsis SOS2 protein kinase physically interacts with and is activated by the calcium-binding protein SOS3. *Proc Natl Acad Sci USA* 97: 3735–3740
- Hasegawa PM, Bressan RA, Zhu JK, Bohnert HJ (2000) Plant cellular and molecular responses to high salinity. *Annu Rev Plant Physiol Plant Mol Biol* 51: 463–499
- Hellendoorn K, Verlaan PW, Pleij CW (1997) A functional role for the conserved protonatable hairpins in the 5' untranslated region of turnip yellow mosaic virus RNA. *J Virol* 71: 8774–8779
- Inan G, Zhang Q, Li P, Wang Z, Cao Z, Zhang H, Zhang C, Quist TM, Goodwin SM, Zhu J, et al (2004) Salt cress: a halophyte and cryophyte Arabidopsis relative model system and its applicability to molecular genetic analyses of growth and development of extremophiles. *Plant Physiol* 135: 1718–1737
- Jacobsen SE, Sakai H, Finnegan EJ, Cao X, Meyerowitz EM (2000) Ectopic hypermethylation of flower-specific genes in Arabidopsis. *Curr Biol* 10: 179–186
- Kant S, Bi YM, Weretilnyk E, Barak S, Rothstein SJ (2008) The Arabidopsis halophytic relative *Thellungiella halophila* tolerates nitrogen-limiting conditions by maintaining growth, nitrogen uptake, and assimilation. *Plant Physiol* 147: 1168–1180
- Kant S, Kant P, Raveh E, Barak S (2006) Evidence that differential gene expression between the halophyte, *Thellungiella halophila*, and *Arabidopsis thaliana* is responsible for higher levels of the compatible osmolyte proline and tight control of Na⁺ uptake in *T. halophila*. *Plant Cell Environ* 29: 1220–1234
- Klaff P, Riesner D, Steger G (1996) RNA structure and the regulation of gene expression. *Plant Mol Biol* 32: 89–106
- Kore-eda S, Cushman MA, Akselrod I, Bufford D, Fredrickson M, Clark E, Cushman JC (2004) Transcript profiling of salinity stress responses by large-scale expressed sequence tag analysis in *Mesembryanthemum crystallinum*. *Gene* 341: 83–92
- Lieth H, Sucre MG, Herzog B, editors (2008) Mangroves and Halophytes. Springer, New York
- Lin H, Yang Y, Quan R, Mendoza I, Wu Y, Du W, Zhao S, Schumaker KS, Pardo JM, Guo Y (2009) Phosphorylation of SOS3-LIKE CALCIUM BINDING PROTEIN8 by SOS2 protein kinase stabilizes their protein complex and regulates salt tolerance in *Arabidopsis*. *Plant Cell* 21: 1607–1619
- Ma J, Devos KM, Bennetzen JL (2004) Analyses of LTR-retrotransposon structures reveal recent and rapid genomic DNA loss in rice. *Genome Res* 14: 860–869
- Meagher TR, Vassiliadis C (2005) Phenotypic impacts of repetitive DNA in flowering plants. *New Phytol* 168: 71–80
- Nah G, Pagliarulo CL, Mohr PG, Luo M, Sisneros N, Yu Y, Collura K, Currie J, Goicoechea JL, Wing RA, et al (2009) Comparative sequence analysis of the SALT OVERLY SENSITIVE1 orthologous region in *Thellungiella halophila* and *Arabidopsis thaliana*. *Genomics* 94: 196–203
- Oh DH, Lee SY, Bressan RA, Yun DJ, Bohnert HJ (2010) Intracellular consequences of SOS1 deficiency during salt stress. *J Exp Bot* 61: 1205–1213
- Oh DH, Leidi E, Zhang Q, Hwang SM, Li Y, Quintero FJ, Jiang X, D'Urzo MP, Lei SY, Zhao Y, et al (2009) Loss of halophytism by interference with SOS1 expression. *Plant Physiol* 151: 210–222
- O'Kane SL Jr, Al-Shehbaz IA (2003) Phylogenetic position and generic limits of Arabidopsis (Brassicaceae) based on sequences of nuclear ribosomal DNA. *Ann Mo Bot Gard* 90: 603–612
- Orsini F, D'Urzo MP, Inan G, Serra S, Oh DH, Mickelbart MV, Consiglio E, Li X, Jeong JC, Yun DJ, et al (2010) A comparative study of salt tolerance parameters in 11 wild relatives of *Arabidopsis thaliana*. *J Exp Bot* 61: 3787–3798
- Poroyko V, Spollen WG, Hejlek LG, Hernandez AG, LeNoble ME, Davis G, Nguyen HT, Springer GK, Sharp RE, Bohnert HJ (2007) Comparing regional transcript profiles from maize primary roots under well-watered and low water potential conditions. *J Exp Bot* 58: 279–289
- Qiu QS, Guo Y, Dietrich MA, Schumaker KS, Zhu JK (2002) Regulation of SOS1, a plasma membrane Na⁺/H⁺ exchanger in *Arabidopsis thaliana*, by SOS2 and SOS3. *Proc Natl Acad Sci USA* 99: 8436–8441
- Quan R, Lin H, Mendoza I, Zhang Y, Cao W, Yang Y, Shang M, Chen S, Pardo JM, Guo Y (2007) SCABP8/CBL10, a putative calcium sensor, interacts with the protein kinase SOS2 to protect *Arabidopsis* shoots from salt stress. *Plant Cell* 19: 1415–1431
- Quintero FJ, Ohta M, Shi H, Zhu JK, Pardo JM (2002) Reconstitution in yeast of the Arabidopsis SOS signaling pathway for Na⁺ homeostasis. *Proc Natl Acad Sci USA* 99: 9061–9066
- Romano PG, Horton P, Gray JE (2004) The Arabidopsis cyclophilin gene family. *Plant Physiol* 134: 1268–1282

- Sanchez HB, Lemeur R, Van Damme P, Jacobsen SE (2003) Ecophysiological analysis of drought and salinity stress of quinoa (*Chenopodium quinoa* Willd.). *Food Rev Int* **19**: 111–119
- Schwartz S, Zhang Z, Frazer KA, Smit A, Riemer C, Bouck J, Gibbs R, Hardison R, Miller W (2000) PipMaker: a Web server for aligning two genomic DNA sequences. *Genome Res* **10**: 577–586
- Shi H, Ishitani M, Kim C, Zhu JK (2000) The *Arabidopsis thaliana* salt tolerance gene SOS1 encodes a putative Na⁺/H⁺ antiporter. *Proc Natl Acad Sci USA* **97**: 6896–6901
- Shi H, Lee BH, Wu SJ, Zhu JK (2003) Overexpression of a plasma membrane Na⁺/H⁺ antiporter gene improves salt tolerance in *Arabidopsis thaliana*. *Nat Biotechnol* **21**: 81–85
- Shi H, Quintero FJ, Pardo JM, Zhu JK (2002) The putative plasma membrane Na⁺/H⁺ antiporter SOS1 controls long-distance Na⁺ transport in plants. *Plant Cell* **14**: 465–477
- Simoes EA, Sarnow P (1991) An RNA hairpin at the extreme 5' end of the poliovirus RNA genome modulates viral translation in human cells. *J Virol* **65**: 913–921
- Sonnhammer EL, Durbin R (1995) A dot-matrix program with dynamic threshold control suited for genomic DNA and protein sequence analysis. *Gene* **167**: GC1–GC10
- Suzuki M, Wang HH, McCarty DR (2007) Repression of the LEAFY COTYLEDON 1/B3 regulatory network in plant embryo development by VP1/ABSCISIC ACID INSENSITIVE 3-LIKE B3 genes. *Plant Physiol* **143**: 902–911
- Swindell WR, Huebner M, Weber AP (2007) Transcriptional profiling of *Arabidopsis* heat shock proteins and transcription factors reveals extensive overlap between heat and non-heat stress response pathways. *BMC Genomics* **8**: 125.1–125.15
- Taji T, Sakurai T, Mochida K, Ishiwata A, Kurotani A, Totoki Y, Toyoda A, Sakaki Y, Seki M, Ono H, et al (2008) Large-scale collection and annotation of full-length enriched cDNAs from a model halophyte, *Thellungiella halophila*. *BMC Plant Biol* **8**: 115.1–115.12
- Taji T, Seki M, Satou M, Sakurai T, Kobayashi M, Ishiyama K, Narusaka Y, Narusaka M, Zhu JK, Shinozaki K (2004) Comparative genomics in salt tolerance between *Arabidopsis* and *Arabidopsis*-related halophyte salt cress using *Arabidopsis* microarray. *Plant Physiol* **135**: 1697–1709
- Vinocur B, Altman A (2005) Recent advances in engineering plant tolerance to abiotic stress: achievements and limitations. *Curr Opin Biotechnol* **16**: 123–132
- Volkov V, Amtmann A (2006) *Thellungiella halophila*, a salt-tolerant relative of *Arabidopsis thaliana*, has specific root ion-channel features supporting K⁺/Na⁺ homeostasis under salinity stress. *Plant J* **48**: 342–353
- Volkov V, Wang B, Dominy PJ, Fricke W, Amtmann A (2004) *Thellungiella halophila*, a salt-tolerant relative of *Arabidopsis thaliana*, possesses effective mechanisms to discriminate between potassium and sodium. *Plant Cell Environ* **27**: 1–14
- Wang B, Davenport RJ, Volkov V, Amtmann A (2006) Low unidirectional sodium influx into root cells restricts net sodium accumulation in *Thellungiella halophila*, a salt-tolerant relative of *Arabidopsis thaliana*. *J Exp Bot* **57**: 1161–1170
- Wang Z, Weber JL, Zhong G, Tanksley SD (1994) Survey of plant short tandem DNA repeats. *Theor Appl Genet* **88**: 1–6
- Wang ZI, Li P, Fredricksen M, Gong ZH, Kim CS, Zhang CQ, Bohnert HJ, Zhu J-K, Bressan RA, Hasegawa PM, Zhao YX, Zhang H (2004) Expressed sequence tags from *Thellungiella halophila*, a new model to study plant salt-tolerance. *Plant Sci* **166**: 609–616
- Weigel D, Mott R (2009) The 1001 genomes project for *Arabidopsis thaliana*. *Genome Biol* **10**: 107.1–107.5
- Wong CE, Li Y, Whitty BR, Díaz-Camino C, Akhter SR, Brandle JE, Golding GB, Weretilnyk EA, Moffatt BA, Griffith M (2005) Expressed sequence tags from the Yukon ecotype of *Thellungiella* reveal that gene expression in response to cold, drought and salinity shows little overlap. *Plant Mol Biol* **58**: 561–574
- Xiong L, Zhu JK (2002) Molecular and genetic aspects of plant responses to osmotic stress. *Plant Cell Environ* **25**: 131–139
- Zhang Y, Lai J, Sun S, Li Y, Liu Y, Liang L, Chen M, Xie Q (2008) Comparison analysis of transcripts from the halophyte *Thellungiella halophila*. *J Integr Plant Biol* **50**: 1327–1335
- Zhu JK (2001) Plant salt tolerance. *Trends Plant Sci* **6**: 66–71
- Zimmermann P, Hirsch-Hoffmann M, Hennig L, Gruissem W (2004) GENEVESTIGATOR: *Arabidopsis* microarray database and analysis toolbox. *Plant Physiol* **136**: 2621–2632
- Zouari N, Ben Saad R, Legavre T, Azaza J, Sabau X, Jaoua M, Masmoudi K, Hassairi A (2007) Identification and sequencing of ESTs from the halophyte grass *Aeluropus litoralis*. *Gene* **404**: 61–69